Choroidal Segmentation and Volume Measurement of Optical Coherence Tomography Images in Eyes using Intensity-Threshold Method

[1]Neeru Rai, [2]John S. Werner and [3]Raju Poddar

[1]Department of Bio-Engineering, Birla Institute of Technology-Mesra, Ranchi, JH 835 215, India.
[2]Vision Science and Advanced Retinal Imaging laboratory, Department of Ophthalmology and Vision Science, University of California Davis, Sacramento, CA 95817, USA
[3]Corresponding author: Department of Bio-Engineering, Birla Institute of Technology-Mesra, Ranchi 835215, India.
Ph.: +91-651-2276223; TeleFax: +91-651-2275401,
Email: rpoddar@bitmesra.ac.in

Abstract— **We present a relatively new and robust method for automated segmentation of choroids in healthy and pathological eyes. The 1μm swept-source optical coherence tomography (OCT) images were utilized for this purpose due to deeper penetration in choroids. The algorithm is build with an intensity-threshold technique. The method is demonstrated on healthy and age related macular degeneration (AMD) patient's eyes. The total choroidal volume is calculated automatically. The results are well correlated with available reports.**

Keyword: **Coherence Tomography, optical biopsy, binarization technique, Gaussian filter.**

I. INTRODUCTION

Optical Coherence Tomography (OCT) is a new emerging technology for biomedical imaging and optical biopsy. It was first demonstrated in the year 1991, for the imaging of internal cross-sectional microstructure of tissues using a low-coherence interferometer system (Fujimoto *et al.* (2000) & Huang *et al.* (1991)). Since its introduction it has found a potential use in the field of retinal imaging to reveal the changes in the morphology of the retina in normal and diseased eyes (Adhi *et al.* (2014)).

Time-domain optical coherence tomography (TD-OCT) was used for retinal imaging but due to its poor resolution and inability to capture 3-D images it sooner got replaced with spectral-domain optical coherence tomography (SD-OCT) systems which provide higher resolution and 3-D imaging possibilities. Swept-source (SS) OCT is now an attractive alternative for 1 μm spectral band OCT (1000-1100 nm) over SD-OCT. Its main advantages include robustness to sample motion, a long measurement range in depth due to short instantaneous line-width, linear sampling in wavenum ber (k-clock–trigger), compactness, increased detection efficiency (balanced detection scheme) and high imaging speed (Michalewska *et al.* (2013), Choma *et al.* (2003) & Wojtkowski (2010)). The use of longer wavelengths helped in deeper light penetration allowing a full depth volumetric imaging of the choroid.

The choroid is the most vascular part of the eye characterized by the region below the RPE and above the chorio-scleral interface. It performs the vital role in supplying the eye with appropriate oxygen and other essential nutrients (Caneiro *et al.* (2013)). A number of diseases affecting the macula, such as age-related

macular degeneration (AMD), polypoidal choroidal vasculopathy (PCV), and central serous chorioretinopathy (CSC), have been found to be correlated to the choroidal dysfunction.

Earlier, a vast majority of studies examining choroidal thickness and volume using OCT instruments have utilized manual segmentation methods, which are time consuming and more prone to subjective error. Recently, a small number of methods have been reported for the fully-automatic segmentation of the choroidal layer. A two-stage statistical model has been used by Kajic *et al.* (2011) to automatically segment out the choroidal region in normal and pathological 1060 nm OCT image. Hu *et al.* (2013) used a graph-based search theory for semi-automatic segmentation of the choroid. Also, Tian *et al.* (2013) used the graph-based search theory for fully-automatic segmentation of the choroid.

In the current, we have implemented a method that uses intensity-threshold based binarization (ITB) technique for the fully automatic segmentation of the choroidal layer. Although the concept is very simple, there are several difficulties in the application of the ITB technique to OCT images mainly because of the depth-dependent signal decay due to scattering in the sample. To avoid this intrinsic problem, en face images will be extracted from a constant distance from the RPE and not from a constant distance from the zero delay point. The signal decay is nearly even in this en face image, hence, the ITB technique can be applied.

II. MATERIALS AND METHODS

A. Imaging System and scanning protocol

SSOCT data sets were obtained in the Vision Science and Advanced Retinal Imaging laboratory (VSRI) at the University of California Davis Medical Center on a 62-year-old healthy subject with normal ocular media and two other AMD patients. Written informed consent was obtained prior to imaging approved by the institutional review board (IRB). The description of SSOCT system was reported in our previous work, Poddar *et al.* (2014), allowing posterior segment imaging. The light source is an external cavity tune-able laser (ECTL), swept-source laser (Axsun Technologies), with a central wavelength of 1060 nm, sweep bandwidth of 110 nm, repetition rate of 100 kHz, 46% duty cycle and average output power of ~23 mW.

The subject's head position was fixed during acquisition using a custom bite-bar and forehead rest. There was no need for pupil dilation. Scanning areas of the retina was 1.5x1.5 mm^2. For the 1.5 x 1.5 mm^2 scanning pattern, 4.2 μm spacing between both consecutive A-scans and BM -scans was used. The A-line exposure time was 7.2 μs and the spectral data were saved in a binary file format for post-processing in custom-made software. All images shown in this manuscript were acquired *in vivo* at 100,000 axial scans (A-scan) rate per second. Each B-scan consisted of 440 A-scans acquired over a 1.5 mm lateral scanning range.

B. Segmentation Algorithm

All the SS-OCT data sets saved in binary format are first imported into FIJI/ImageJ, 2014 software for registration of the B-Scans contained in the volumetric scan. It helps in aligning all the frames of the volume scans into the same coordinate system. Then, the images are imported into the custom-made software for the segmentation of the choroid using ITB technique for the segmentation purpose. For the segmentation, here we have utilized a method similar to that presented by Yasuno *et al*. (2006). Two boundaries namely, anterior and the posterior boundary were extracted. The anterior boundary is represented by the outer segment of a highly reflective layer of RPE (the Bruch's membrane).

To suppress the imaging noise the OCT images are passed through a Gaussian filter having a standard deviation radius of 2 (i.e. σ = 2) for smoothing of the edges. The thresholding data is obtained by the iterated measurement of the histogram of the image. The histogram result is then divided into four groups. The group of pixels corresponding to the highest intensities is used for thresholding of the gradient magnitude images which yields the binary images. The small particles in the binary image are removed by using a 3 x 3 erosion process. This resulting binary image represents the RPE layer whose edges are found by using differentiation method by 2 x 2 matrix. The segmented line was obtained from the matrix.

C. Choroidal volume determination

In the segmented image, the area between the upper and lower edges of the choroid was calculated from OCT volume scan. Each pixel dimension was first converted to actual physical dimension of image (image scanning length divided by the corresponding number of total number of pixel). The number obtained was then multiplied by the total number of pixels present in the segmented choroid region. This gives the

area of the choroid of a single B-scan. Then the area of all the B-scans in a volumetric scan is summed-up to determine the cumulative volume.

III. RESULTS AND DISCUSSION

The acquired OCT images were segmented to reveal chorio-retina and choroid-sclera interface. Figure 1 shows the results for the healthy subject. The left panel A(a) and A(c) shows the unsegmented OCT images whereas the right panel A(b) and A(d) shows the OCT images after segmentation. The line pointed by the yellow arrow is Chorio-retinal interface and the line pointed by the green arrow refers to the choroid-sclera interface. The region between these two lines represents the choroid region of the eye. The cumulative volume of the choroidal region was found to be 22.90477 mm^3 (Caneiro *et al.* (2013) & Kajic *et al.* (2011)).

Similarly, Figure 2 and Figure 3 demonstrate the OCT images before and after the segmentation of the two AMD patients. The yellow arrow points to the chorio-retinal interface and the green arrow to the choroid-sclera interface. The OCT images of the AMD patient shows the irregular RPE layer as can be seen in the form of certain peaks. But the automated segmentation introduced by us demonstrates a robust method to easily segment the peak regions also.

The cumulative volume for AM D patient-1 is found to be 22.03656 mm^3 and for patient-2 it is 23.13005 mm^3, see Table 1. The results were well correlated with existing report of Caneiro *et al.* (2013) & Kajic *et al.* (2011).

TABLE I. CUMULATIVE CHOROIDAL THICKNESS AND VOLUME OF NORMAL AND DISEASED SUBJECTS

Subjects	Choroidal Area (mm^2)	Cumulative Choroidal Volume (mm^3)
Normal	0.34651	22.90477
AM D patient-1	0.24701	22.03656
AM D patient-2	0.46989	23.13005
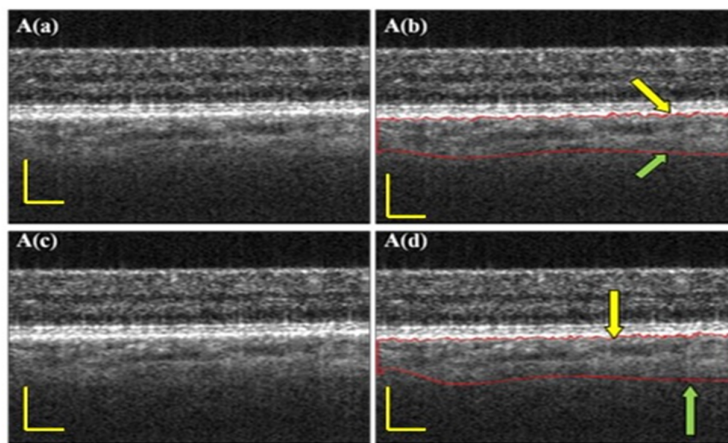
Figure 1. SS-OCT images of healthy posterior segment eye with 3° temporal eccentricity from fovea. A(a) and A(c):original OCT image (without segmentation), A(b) and A(d):demonstrates segmented choroidal layer represented by the lines between the arrows, (yellow arrow: boundary between retina and choriod; green arrow: boundary between choriod and sclera). Scale bar: 300 µm

IV. CONCLUSION

A new and robust algorithm for automatic segmentation of anterior and posterior choroidal boundaries is demonstrated. The method uses an Intensity-threshold based binarization technique to segment the two boundaries. The choroid sclera interface was detected at a constant depth from the RPE layer. The approach is tested and evaluated on different data sets of normal and pathological subjects. The algorithm shows high accuracy in case of AMD patients also with deformed RPE layer. The fully automated segmentation method developed here provides many medically essential histopathological findings in the field of ophthalmology.
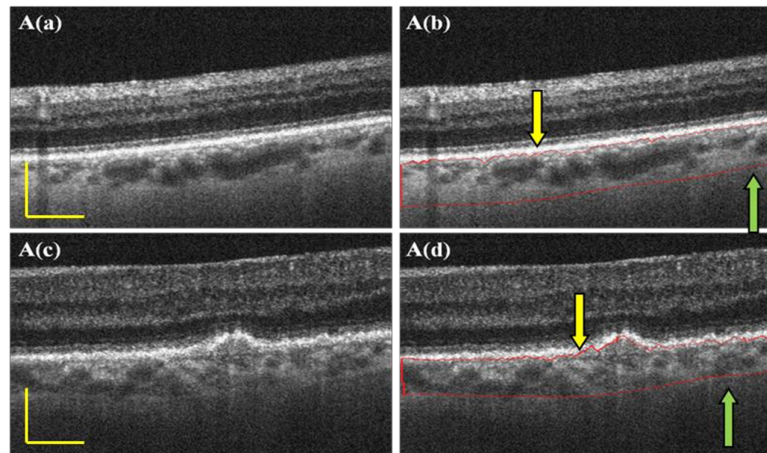
Figure 2. SS-OCT images of posterior eye of 1st AMD patient. A(a) & A(c):original OCT image, A(b) & A(d):demonstrates segmented choroidal layer represented by lines between the arrows. (yellow arrow: boundary between retina and choriod; green arrow: boundary between choriod and sclera). Scale bar: 300 μm
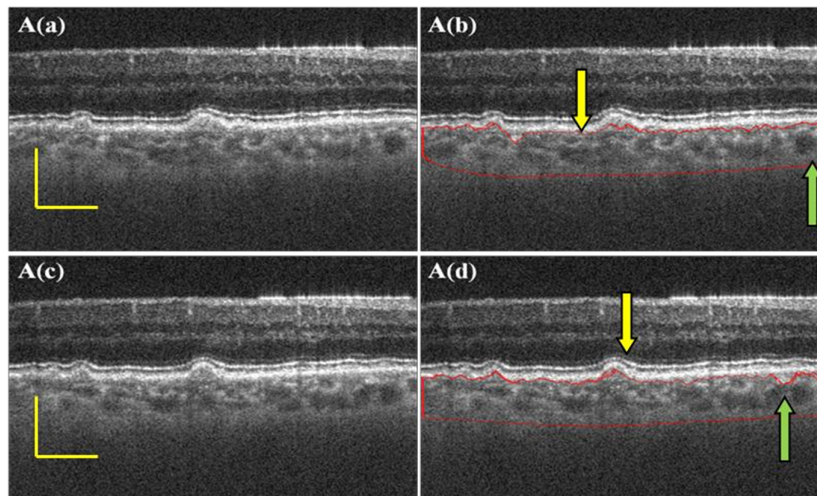
Figure 3. SS-OCT images of posterior eye of 2nd AMD patient. A(a) & A(c):original OCT image, A(b) & A(d):demonstrates segmented choroidal layer represented by lines between the arrows. (yellow arrow: boundary between retina and choriod; green arrow: boundary between choriod and sclera). Scale bar: 300 μm

REFERENCES

[1] Adhi M., Liu J. J., Qavi A. H., et al. (2014), "Choroidal analysis in healthy eyes using Swept-source optical coherence tomography compared to spectral domain Optical coherence tomography", American Journal of Ophthalmology 157, 1272-1281.

[2] Caneiro D. A., Read S. A., & Collins M. J. (2013), "Automatic segmentation of choroidal thickness in Optical coherence tomography", Biomedical Optics Express 4(12)**,** 2795-2812.

[3] Choma M. A., Sarcenic M. V., Yang C., et al. (2003), "Sensitivity advantage of swept source and fourier domain OCT", Optics Express 11(18), 2183-2 190.

[4] Fujimoto J. G., Pitris C., Boppart S. A., et al (2000)., "Optical coherence Tomography: An emerging technology for biomedical imaging and optical biopsy", Nature America 2(1-2), 9-25.

[5] H uang D., Swanson E. A., Li n C. P., et al. (1991), "Optical coherence tomography", Science 254(5035), 1178-1181.

[6] Hu Z., Wu X., Ouyang Y., et al. (2013), "Semi-automated segmentation of the choroid in spectral-domain Optical Coherence Tomography volume scans", Investigative Ophthalmology and Visual Science 54(3), 1722-1729.

[7] K aji c V., Esm aeel pour M., Povazay B., et al. (2011), "Automated choroidal segmentation of 1060nm Optical coherence tomography in healthy and pathologic eyes using a statistical model", Biomedical Optics Express 3(1), 86-103.

[8] Michalewska Z., Michalewski J., & Nawrocki J. (2013), "Swept source Optical coherence tomography", Retina today, 50-56.

[9] Poddar R., K i m D. Y., Werner J. S., et al. (201 4), "In vivo imaging of human vasculature in chorioretinal complex using phase variance contrast method with phase stabilized 1 μm Swept-source Optical coherence tomography", Journal of Biomedical Optics, 1-12.

[10] Schindelin, J.; Arganda-Carreras, I. & Frise, E. et al. (2012), "Fiji: an open-source platform for biological-image analysis", Nature methods **9(7)**: 676-682

[11] Ti an J., M arzi li ano P., B askaran M., et al. (2013), "Automatic measurements of choroidal thickness in ED I-OCT images", Biomedical Optics express 4(3), 397-411.

[12] Wojtkowski M. (2010), "High speed optical coherence tomography:basics and applications", Applied optics 49(16), D30-D61.

[13] Yasuno Y., M akita S., Hong Y., et al. (2006), "Optical coherence angiography", Optics Express 14(17), 7821-7840.